Published in final edited form as:
*J Proteomics*. 2013 January 14; 78: 172–187. doi:10.1016/j.jprot.2012.11.013.

# Protein expression profiles of human lymph and plasma mapped by 2D-DIGE and 1D SDS–PAGE coupled with nanoLC–ESI–MS/MS bottom-up proteomics

**Cristina C. Clement**[a], **David Aphkhazava**[a], **Edward Nieves**[b], **Myrasol Callaway**[a], **Waldemar Olszewski**[d], **Olaf Rotzschke**[e], and **Laura Santambrogio**[a,c,*]

Laura Santambrogio: laura.santambrogio@einstein.yu.edu

[a]Department of Pathology, Albert Einstein College of Medicine, Bronx, NY 10461, USA [b]Department of Developmental and Molecular Biology, Albert Einstein College of Medicine, Bronx, NY 10461, USA [c]Department of Microbiology and Immunology, Albert Einstein College of Medicine, Bronx, NY 10461, USA [d]Department of Surgical Research and Transplantology, Polish Academy of Sciences, Warsaw 00950, Poland [e]Singapore Immunology Network (SIgN), Agency for Science, Technology and Research (A*STAR), 8A Biomedical Grove #04-06, Immunos 138648, Singapore

## Abstract

In this study a proteomic approach was used to define the protein content of matched samples of afferent prenodal lymph and plasma derived from healthy volunteers. The analysis was performed using two analytical methodologies coupled with nanoliquid chromatography-tandem mass spectrometry: one-dimensional gel electrophoresis (1DEF nanoLC Orbitrap–ESI–MS/MS), and two-dimensional fluorescence difference-in-gel electrophoresis (2D-DIGE nanoLC–ESI–MS/MS). The 253 significantly identified proteins ($p<0.05$), obtained from the tandem mass spectrometry data, were further analyzed with pathway analysis (IPA) to define the functional signature of prenodal lymph and matched plasma. The 1DEF coupled with nanoLC–MS–MS revealed that the common proteome between the two biological fluids (144 out of 253 proteins) was dominated by complement activation and blood coagulation components, transporters and protease inhibitors. The enriched proteome of human lymph (72 proteins) consisted of products derived from the extracellular matrix, apoptosis and cellular catabolism. In contrast, the enriched proteome of human plasma (37 proteins) consisted of soluble molecules of the coagulation system and cell–cell signaling factors. The functional networks associated with both common and source-distinctive proteomes highlight the principal biological activity of these immunologically relevant body fluids.

### Keywords

Lymph; Plasma; Proteomic; Biomarkers; 2D-DIGE; NanoLC–ESI–MS/MS



*Corresponding author at: Departments of Pathology, Microbiology and Immunology, Albert Einstein College of Medicine, NY, USA. Tel.: +1 718 430 3458.

Supplementary data to this article can be found online at http://dx.doi.org/10.1016/j.jprot.2012.11.013.

## 1. Introduction

The peripheral pre-nodal lymph is formed in the interstitial space around the capillary beds as a result of a filtration process driven by the hydrostatic pressure in the arterial end of capillaries. This hydrostatic pressure forces fluids and proteins into the extracellular space. A small fraction of this extracellular fluid returns to the capillary in response to intra-vascular osmotic pressure while the bulk of the extravasated fluids and proteins form the lymph that collects into an open-ended network of lymphatic capillaries present in every parenchymal organ. The lymphatic capillaries merge into progressively bigger vessels that transport the pre-nodal lymph to nodes disseminated throughout the body [1]. The afferent lymphatics perforate the lymph node capsule and enter into the sub-capsular sinuses. From these sinuses, particulate material and molecules with a molecular weight above 100 kDa travel peripherally in the sub-cortical space into the medullary sinuses and then into efferent lymphatic vessels. In this way bacteria and high molecular weight molecules are either: captured by macrophages and dendritic cells present in the sub-capsular and medullary sinuses; or exit the lymph-node and reach additional nodal stations through the efferent lymphatic, ensuring that pathogens are captured in nodal stations and do not enter the blood [1,2]. Molecules smaller then 80–100 kDa percolate from the sub-capsular sinuses into a series of channels (known as the conduit system) that are in direct contact with the dendritic cell network of T cell areas. From the conduit the lymph will then proceed to the high endothelial venules in the nodal sinus. As such, lymph nodes collect and filter lymphatic fluid-carried antigens from every parenchymal organ and tissue. In the nodes, self and non self antigens, will be presented by antigen presenting cells with the ultimate goal of maintaining peripheral self-tolerance as well as inducing immunity to invading pathogens [3,4].

The immunological importance of the lymph has been recognized for some time, but its characterization has been elusive due to the difficulty of collecting samples from the lymphatics, which run deeper than blood vessels. Thus, relatively little is known about the extent to which the protein content of human lymph compares with that of plasma. Until recently the dominating notion was that the proteomic profile of pre-nodal afferent lymph mostly overlapped with that of plasma, since the former was considered to be an ultra filtrate of the latter, albeit with a concentration anticipated to be lower in lymph compared to plasma. However, this notion was challenged by a few comparative analyses of lymph and plasma, which reported the presence of specific proteins in one fluid but not the other [5–8]. More recently, proteomic analysis from lymph collected from sites of sterile or pathogen-induced inflammation also indicated the presence of several tissue specific proteins [5–13]. In our own studies we found that a difference between these two biological fluids was the presence of a soluble peptidome/degradome in the lymph, in higher amounts then the one found in the plasma [13]. These results led us to propose the hypothesis that since the lymph directly circulates in each parenchymal organ, it collects products derived from their metabolic/catabolic activity, forming an enriched lymph proteome derived from many cellular compartments, which, albeit already reported in the plasma [14], could be over-expressed in the lymph [13].

In order to investigate this hypothesis we have performed a comprehensive proteomics analysis of afferent pre-nodal lymph and matched plasma samples derived from healthy donors. The analysis was carried out using two proteomics strategies: 1D gel LC–ESI–MS/MS analysis, and two dimensional fluorescence difference in gel electrophoresis (2D-DIGE) coupled with nanoLC–ESI–MS–MS on a Orbitrap and LTQ mass spectrometer. Pathway analysis (IPA) was utilized to compare the proteome of the two biological fluids in a functional and statistically relevant manner.

The biological fluid consisted of matched lymph and plasma, pooled from eighteen subjects, as well as, nine individual lymph and matched plasma samples. The identified lymph and plasma proteins overlapped by more than 85% between the pooled and individual subject samples. The remaining 15% of the proteome contained hits retrieved either only from the pooled lymph samples or from the individual ones. A total of 144 proteins were found to be common between the plasma and lymph, represented mainly by complement activation and blood coagulation components, transporters and protease inhibitors. The enriched proteome of human lymph (*72* proteins), collected from the lower limbs, consisted of products derived from the extracellular matrix and cellular catabolism. In contrast, the enriched proteome of human plasma (37 proteins) consisted of soluble molecules of the coagulation system and cell–cell signaling factors.

The global comparative proteomic analysis of human lymph and plasma presented herein represents the first step towards advanced studies which could lead to the identification and validation of selective biomarkers of the prenodal lymph.

## 2. Materials and methods

### 2.1. Reagents

Trifluoroacetic acid, acetonitrile, acetic acid, formic acid, methanol (99% purity, HPLC grade) were purchased from Fisher Scientific (Pittsburgh, PA, USA). Porcine trypsin (20 μg, specific activity>5000 units/mg seq. grade modified) was purchased from Promega (Madison, WI, USA). Urea, thiourea, octylglucoside, dithiothreitol (DTT), iodoacetamide, ammonium bicarbonate, Coomassie Brilliant Blue R-250, KCl, $KH_2PO_4$, $H_3PO_4$ and $Na_2CO_3$ were purchased from SIGMA (St. Louis, MO, USA). Complete TM Proteinase inhibitor cocktail was purchased from Santa Cruz Biotechnology (Santa Cruz, CA, USA). The AurumTM Serum protein Mini Kit (Cat #732-6701) for depletion of immunoglobulins IgG and albumin in plasma and lymph was purchased from BIORAD.

**2.1.1. Collection of pre-nodal lymph and plasma—**Lymph and plasma samples were collected from eighteen healthy males (22 to 36 years old). All subjects were given a full medical examination to exclude recreational drug abuse and cardiovascular, liver, renal, endocrine and hematologic diseases. No subject was under a special diet or medication. Alcohol was avoided for 48 h before and during the study. The study was approved by the Royal London School of Medicine Committee for Clinical Investigation and by the Albert Einstein College of Medicine, Committee for Clinical Investigation. All subjects gave informed written consent. Prenodal peripheral lymph was collected as previously described [13]. A blood sample from each subject was also drawn. Blood and lymph samples were centrifuged at 1500 g for 15 min at 4 °C within 20 min of collection and the supernatants transferred to polypropylene microcentrifuge tubes [14]. Samples were all supplemented with a cocktail of proteases inhibitors (Roche).

**2.1.2. Albumin and IgG depletion of lymph and plasma—**Total protein concentration from human plasma and lymph was determined using the Bradford assay (Biorad reagent). IgG and albumin depletion was performed using Aurum Serum spin columns from Biorad pre-packed with a mixture of Affi-Gel Blue and Affi-Gel protein A according to the manufacturer's instructions [15–17]. Eluted fractions were used for further 1D gel or 2D-DIGE electrophoresis.

**2.1.3. 2D DIGE protein expression profiling of human lymph and plasma—**Five hundred micrograms of protein from whole lymph and plasma, depleted of IgG and albumin, were purified with a 2-D Clean-up Kit (GE Healthcare BioSciences, Little Chalfont, UK), quantified with the 2-D Quant Kit, and labeled with CyDye DIGE Fluors [18–21]. 100 μg of

proteins from the depleted lymph and plasma were labeled with 400 pmol of each of the dyes (Cy3 for plasma and Cy5 for lymph). After incubating on ice for 30 min in the dark, the labeling reaction was stopped with 10 mM lysine. For each gel, Cy3- and Cy5-labeled proteins were mixed with 450 μL rehydration buffer (7 M urea, 2 M thiourea, 4% (w/v) CHAPS, 40 mM DTT, 1% IPG buffer (pH 4–7), 0.002% (w/v) Bromophenol blue) (Applied BIOMICS Inc. facilities, Hayward, CA). The labeled protein mixture was applied to Immobiline DryStrip strips (24 cm, pH 4–7; GE Healthcare). Isoelectric focusing (IEF) was performed with an Ettan IPGphor II apparatus (GE Healthcare) at 30 V for 12 h, 500 V for 1 h, 1000 V for 1 h, and 10,000 V for up to a total of 85,000 Vh. After IEF, the proteins were reduced and alkylated by successive 15 min treatments with equilibration buffer containing 2%(w/v) DTT followed by 2.5% (w/v) iodoacetamide. The proteins were then resolved in 4–20% SDS–PAGE gels using an Ettan DALTsix instrument (GE Healthcare). For MS analysis, 500 μg unlabeled pool protein were run in parallel on a preparative gel and stained with Deep Purple (GE Healthcare) according to the manufacturer's instructions (performed at Applied BIOMICS Inc. facilities, Hayward, CA). Gel image were acquired on a Typhoon 9400 scanner (GE Healthcare) and analyzed using DeCyder Software (V6.0, GE Healthcare) as described previously [13–18]. The protein expression patterns of human lymph were compared with those of matched plasma, respectively. The ratios of protein abundance that increased or decreased more than 3.0-fold (*t*-test and ANOVA, $p<0.01$) were considered significant. 3D view of individual spots was generated with DeCyder (v6.0, GE Healthcare). Protein spots with differences of more than three fold were picked for MS/MS analysis.

**2.1.4. 1D SDS PAGE and in-gel trypsin digestion—**70 μg from each albumin and IgG depleted plasma and lymph sample were run on a 4–20% or 10% SDS–PAGE. Proteins were stained with Coomassie/Colloidal Brilliant Blue R-250 and 16 gel bands were cut across the whole lymph and plasma sample lane. Each band was excised further into smaller pieces (~1×2 mm) and placed into a 0.65 mL micro-centrifuge siliconized tube (PGC Scientific) and washed with 250 μL of Millipore water twice for 5 min. Gel pieces were washed three times each with 25 mM $NH_4HCO_3$ in 50% acetonitrile, dried in a SpeedVac, reduced at 56 °C for 1 h with 10 mM DTT in 25 mM $NH_4HCO_3$ and alkylated for 45 min at RT with 55 mM iodoacetamide in 25 mM $NH_4HCO_3$. Gel pieces were then washed with 25 mM $NH_4HCO_3$ for 10 min and dehydrated with 25 mM $NH_4HCO_3$ in 50% acetonitrile for 5 min. Following drying in a SpeedVac, the gel pieces were mixed with 12.5 ng/μL of trypsin and incubated on ice for 40 min in 25 mM $NH_4HCO_3$. Tryptic digestion was carried out at 37 °C overnight. Tryptic peptides were extracted from the gel using 60% acetonitrile and 0.2% TFA. Following 20 min of vortex and 5 min of sonication, the supernatant was collected and saved. The extraction was repeated once and all the supernatants were combined. After evaporation of acetonitrile in a SpeedVac, the samples were desalted and concentrated with a C18 ZipTip (Millipore) and half of the eluate was analyzed with nanoLC–ESI–MS/MS.

## 2.2. NanoLC–ESI–MS/MS analysis of tryptic peptides

Two independent nanoLC MS/MS methods were employed for the ESI tandem MS/MS sequencing of the peptides derived from the in gel tryptic digests of each of the 1DEF band. In one set of experiments, both the pooled eighteen and the individual patients samples were subjected to the nanoLC–ESI–MS/MS analysis performed on a Ultimate Plus nano-HPLC system with a Famos autosampler (Dionex Corporation, Sunnyvale, CA) and a linear ion trap mass spectrometer (LTQ, Thermo, San Jose, CA) interfaced with a TriVersa NanoMate nanoelectrospray ionization source (Advion BioSciences, Ithaca, NY). In another set of experiments we used the nanoLC/MS/MS with a Waters NanoAcquity HPLC system interfaced to a ThermoFisher Orbitrap Velos Pro in order to gain a higher coverage of the low abundance protein antigens. In the case of the LTQ ESI, the peptides were loaded on a

C18 μ-PrecolumnTM Cartridge (5 μm, 100 Å, 300 μm i.d.×5 mm) by the autosampler with a 25 μL sample loop at a flow rate of 15 μL/min. Mobile phase A was 2% acetonitrile and 0.1% formic acid in water and mobile phase B was 80% acetonitrile and 0.1% formic acid in water. The HPLC flow rate used was 250 nL/min. After injection of 25 μL of sample, and washing for 20 min with 100% mobile phase A, the precolumn was switched in line with the analytical column, C18 PepMap100, 3 μm, 100 Å, 75 μm i.d.×150 mm (Dionex Corporation, Sunnyvale,CA).Then mobile phase B was increased from 2 to 55% over 70 min, held for 5 min, increased to 95% over 20 min and held at 95% B for 5 min. The four most intense ions having a charge state between +2 to +4, determined from an initial survey scan from 300 to 1800 m/z, were selected for zoom scan and MS/MS. In some nanoLC–ESI–MS/MS experiments, the ten most intense ions from each initial MS survey were selected for MS/MS. MS/MS was performed using an isolation width of 2 *m*/z; normalized collision energy of 35% and a minimum signal intensity of 1000 counts. Dynamic exclusion was enabled, such that once a certain ion is selected twice for MS/MS within 30 s, this ion is excluded from being selected again for MS/MS during the next 120 s. When the samples were analyzed with the nanoLC–ESI Orbitrap mass spectrometer, the peptides were loaded on a trapping column and eluted over a 75 μm analytical column at 350 nL/min; the columns were packed with Jupiter Proteo resin (Phenomenex). The injection volume was 30 μL. The mass spectrometer was operated in data-dependent mode, with MS performed in the Orbitrap at 60,000 FWHM resolution (at m/z 400) and MS/MS performed in the LTQ. The fifteen most abundant ions were selected for MS/MS. The peptides derived from the in-gel tryptic digests of the 2D DIGE spots were subjected to sequencing using only the nanoLC–ESI–MS/MS on LTQ system.

**2.2.1. Protein database search of MS/MS spectra—**Proteome Discoverer (version 1.3; Thermo Scientific) [22] was used to generate the mgf files from the raw data generated by the nanoLC Orbitrap and LTQ systems. All mgf files were searched against the human (*Homo sapiens*) NCBInr database (May 27, 2011) with Mascot, in-house, (Matrix Science, London, UK; version 2.3.02). In addition, the mgf files were searched against human (Homo sapiens) (20,266 sequences) in Swiss Prot, version 57.15 (515,203 sequences; 181,334,896 residues). The combined search from NCBI and Swiss Prot was used to generate the final protein IDs. The “Exponentially Modified Protein Abundance Index” (emPAI), which offers approximate, label-free, relative quantization of the proteins in a mixture based on protein coverage by the peptide matches in a database search result [22,23] was extracted only for the 2D-DIGE data for the spots which were characterized by a four fold up-regulation index of the protein expression in the lymph vs. plasma.

A false discovery rate (FDR) for peptide identification was assessed by decoy database searching [22] and was finally adjusted to less than 1.0% for proteins and peptides. The following parameters were used for all searches: trypsin; 1 missed cleavage; variable modifications of carbamidomethylation (Cys), deamidation (Asn and Gln), oxidation (Met, Pro, Lys, Arg); monoisotopic masses; peptide precursor mass tolerance of 1.5 Da; and product ion mass tolerance of 0.5 Da (for the data produced with the LTQ). The mgf files derived from the Orbitrap analysis were searched with the same criteria stated above and assigning a peptide precursor mass of 10 ppm and product ion mass tolerance of 0.8 Da.

Proteins were considered identified having at least one bold red (BR) significant peptide with an ion score cut-off of 45 or greater (corresponding to $p \leq 0.05$ and a FDR proteins ≤1.0% for the data derived from the LTQ) [23]. In the case of the hits retrieved from the Orbitrap data, proteins were considered identified having at least one bold red (BR) significant peptide with an ion score cut-off of 28 or greater (corresponding to $p < 0.05$ and FDR proteins <1.0%) [24,25]. For those proteins identified by only one significant BR peptide the tandem mass spectrometry spectra were checked manually to meet the following

criteria: the difference between the measured and theoretical peptide precursor mass is within 100 or 10 ppm (for LTQ or Orbitrap respectively); MS/MS product ions are within 0.5 Da of the predicted b and y ions; and 80% of the high intensity product ions matched to either b or y ions; and both b and y ions matched [26,27]. A BLAST search against all species was performed with the single peptide hits and only those matching to proteins with an expectation value of $10^{-4}$ and less were included in the results.

### 2.3. Pathways analysis

Ingenuity Pathways Analysis (IPA) software (Ingenuity Systems, CA) was used to investigate the functional aspects of the identified proteins listed in Tables 1 (A and B) (from 2D-DIGE analysis) and Supplement Table 2. The putative interactions among all the identified proteins in the common proteome shared by the human lymph and plasma, and the up-regulated proteome of the lymph (from 2D-DIGE analysis) were analyzed using the statistical significance built-in the software ($p \leq 0.05$) and the new functional networks associated with the given set of proteins molecules were retrieved together with their related interactive pathways.

### 2.4. Western blot analysis

Proteins (70 μg per lane from both lymph and plasma samples, albumin and IgG immunodepleted) were separated by 1D SDS–PAGE on 4–20% bisacrylamide gel and transferred electrophoretically to a nitrocellulose membrane (0.45 μm, from Bio-Rad, Hercules, CA). The membranes were stained with 1% Ponceau S in 5% acetic acid to confirm proper transfer and the equal loading of the two biologically distinctive samples. For destaining, the blot was washed with alkaline water and equilibrated with phosphate buffer saline (PBS). Blocking was performed for 1 h at room temperature in 5% nonfat dried milk, in 100 mM PBS. All incubations with primary antibodies were performed overnight at 4 °C in 100 mM PBS containing 0.5% Tween 20. The following primary antibodies were used to validate the 20 proteins expressed in human lymph and plasma: anti-actin (H-300), rabbit polyclonal (Santa Cruz Biotechnologies Inc., Santa Cruz, CA, Cat. # sc-10731), anti-annexin 6 (G-10) mouse monoclonal, (Santa Cruz Biotechnologies Cat. # sc-166807), anti-cartilage oligomeric protein (COMP) mouse monoclonal purified MaxPab, (Abnova, Cat# H00001311-B01P), anti-collagen type I, mouse monoclonal, (Calbiochem, Cat# I-875), anti-cystatin A, mouse monoclonal (Abcam, Cat#ab10442), anti-cystatin C (C-27) mouse monoclonal, (Santa Cruz Biotechnologies Inc., Cat. # sc-73878), anti-caspase 14 (C-12), mouse monoclonal, (Santa Cruz Biotechnologies Inc., Cat. # sc-48395), anti-calmodulin (CAM) (G-3), mouse monoclonal, (Santa Cruz Biotechnologies Inc., Cat. # sc-137079), anti-ECM1 (F-1) (extracellular matrix protein 1), mouse monoclonal, (Santa Cruz Biotechnologies Inc., Santa Cruz, CA, Cat. # sc-365335), anti-galectin 7 (G-3), mouse monoclonal, (Santa Cruz Biotechnologies Inc., Santa Cruz, CA, Cat. # sc-137085), anti-gelsolin (N-18), goat polyclonal (Santa Cruz Biotechnologies Inc., Santa Cruz, CA, Cat.# sc-6406), anti-GAPDH, rabbit polyclonal, (Abcam, Cat#ab9485), anti-histone H2B (N-20), goat polyclonal (Santa Cruz Biotechnologies Inc., Santa Cruz, CA, Cat. # sc-8650), anti-histone H1(AE-4), mouse monoclonal (Santa Cruz Biotechnologies Inc., Santa Cruz, CA, Cat. # sc-8030), anti-Hsp70/anti-Hsc-70 (H-300), rabbit polyclonal, (Santa Cruz Biotechnologies Inc., Santa Cruz, CA, Cat. # sc-33575), anti-lumican (LUM), rabbit polyclonal, (Proteintech, Cat#10677-1-AP), anti-Pin4 (F-13), mouse monoclonal, (Santa Cruz Biotechnologies Inc., Santa Cruz, CA, Cat. # sc-100810), anti-ribosomal L22 (D-7), mouse monoclonal, (Santa Cruz Biotechnologies Inc., Santa Cruz, CA, Cat. # sc-373993), anti-tetranectin (1DE3), mouse monoclonal, (Santa Cruz Biotechnologies Inc., Santa Cruz, CA, Cat. # sc-80594) and anti-ubiquitin (Ub) (PAD1), mouse monoclonal, (Santa Cruz Biotechnologies Inc., Santa Cruz, CA, Cat. # sc-8017). Secondary antibodies were: peroxidase-conjugated mouse anti-rabbit, affinity purified IgG (H+L), (Jackson-

ImmunoResearch Laboratories Inc., Cat# 111-035-144), bovine anti-goat IgG-HRP, (Santa Cruz Biotechnologies Inc., Santa Cruz, CA, Cat. # sc-2378), or with stabilized peroxidase conjugate anti-mouse (H+L), (Thermo Scientific, Rockford, IL, Cat. # 32430). West Pico enhanced chemiluminescence kit (Thermo Scientific, Rockford, IL), was utilized to visualize proteins (ChemiDoc XRS gel documentation system (Bio-Rad, Hercules, CA)).

## 3. Results

The primary hypothesis that initiated this investigation was that the lymph could potentially carry a wider antigenic repertoire than the plasma and be a richer source of tissue specific self antigens. Fluid from the lymph directly originates from the extracellular milieu where products of tissue catabolism, tissue remodeling, cellular apoptosis, and extracellular matrix processing are pooled before being transported to the draining lymph nodes [14,28].

Two integrated approaches were utilized to analyze proteomic differences between human lymph and plasma; two-dimensional fluorescence difference in gel electrophoresis (2D-DIGE) and 1D SDS–PAGE both coupled with nanoLC– ESI–MS/MS analysis of in gel trypsin-digested proteins. 2D-DIGE allowed the semi-quantitative analysis between the two samples, lymph and plasma, highlighting the upregulated/downregulated proteins in each of the two biological fluids. In addition, the 2D DIGE method enabled a qualitative display of the possible posttranslational modifications and the processed forms of the representative proteomes. However, this technique is limited by the quantity of protein that can be visualized on the gel as well as by the ability to resolve proteins with a pI higher than 11.0 and a MW higher than 120 kDa or below 7 kDa [27]. On the other hand, the 1D SDS–PAGE became the preferred method for the separation of biological fluids, secretomes and subcellular organelles, and provides a global representation of proteomic content which enables a better comparison of the composition of the two biological samples [29–34].

### 3.1. 2D-DIGE and MS/MS identification of proteomic expression profile in human lymph and plasma

Equal amount (100 μg determined from the quantitative Bradford assay) of plasma and lymph proteins (depleted of albumin and IgG) were labeled with Cy3 and Cy5 dye respectively, for 2D-DIGE analysis. Representative 2D-DIGE gels image are shown in Fig. 1A and B along with proteins spots with significant differences in Cy3 to Cy5 fluorescence (Fig. 1B, C, Supplement Fig. 1). Nineteen protein spots with a lymph/plasma ratio above 4.2 were selected for in-gel trypsin digest and nanoLC–MS/MS sequencing for protein identification. Table 1 list all the significant identified proteins from selected 2D DIGE spots as determined by nanoLC– ESI–MS/MS analysis. Positive hits corresponded to Mascot scores ≥45 (at least 1 peptide/hit) plus the fulfillment of the criteria stated in the Materials and methods ($p \leq 0.05$). The proteins significantly up-regulated in the lymph as compared to plasma were (numbers in parenthesis represent Cy3/Cy5 ratio and spot number): calmodulin like protein-5 (epidermal calmodulin), cystatin A, caspase-14 (+28.4; spot 20a), S-100 Ca++ binding proteins S100-A9, A8, calmodulin-like protein 5 (epidermal calmodulin), serpin B3, galectin 7, actin-cytoplasmatic 1 (+14.1; spot 20c), BAI-1 associated protein 2 (+11.5; spot 90), olfactory receptor 2 T35 (+9.4 spot 78), calmodulin like protein 5 (epidermal calmodulin) and cystatin A (+9.4, spot 20b), and vitamin D binding protein (+8.9; spot 47). Also significantly up-regulated were C-type lectin domain family 3B (tetranectin) (+8; spot 75), galectin 7, fatty acid binding protein epidermal, heat shock protein beta-1, annexin 1 (+7.5; spot 30), haptoglobin and cathepsin Z (+6.6; spot 61), BAI-1 associated protein 2 (+6.0; spot 84), gelsolin (+5.4; spot 3), caspase 14, dermicidin, transthyretin, and S100-A7, A8 and A9 (+5.6, spot 18) (Table 1, Fig. 1B).

emPAI values for spots, with at least a four fold up-regulation in lymph vs plasma (Table 1 A and B) are reported. The higher the emPAI, the higher is the expected contribution of a specific protein hit to the volume of the selected spot, and thus to the reported level of fluorescence expression index.

Nano LC–ESI–MS/MS analysis was performed on 16 additional spots that were confirmed from three separate experiments as having at least a 3.0 fold change in their fluorescence protein expression index (defined as the ratio of lymph/plasma, Cy3/Cy5) (Fig. 1B and Supplement Table 1). Among the proteins identified in these spots, several were already previously described in the sheep and rodent lymph [11–13,35], and recently in the human mesenteric lymph (43): alpha-1 antitrypsin, apolipoprotein B precursor, complement factor B, plasminogen, complement component 3, complement protein C7, gelsolin, haptoglobin, fibrinogen alpha A, fibrinogen gamma chain, immunoglobulin gamma heavy chain, lactoferrin, transferrin, among others (Supplement Table 1). Many of these proteins were also shown to be present in more than one spot, probably due to differential posttranslational modifications or partial processing. Additionally, some of the differentially expressed proteins (alpha-1-antitrypsin, vitamin D binding protein, fibrinogen gamma chain, angiotensinogen, C4B3, complement factor B, haptoglobin, apolipoprotein L1, alpha-2-antiplasmin precursor, lipoprotein CIII) separate on the 2D-DIGE with a different MW and pI from the predicted ones, possibly due to partial catabolic processing (Table 1 and Supplement Table 1).

### 3.2. 1-D SDS–PAGE and nanoLC–ESI–MS/MS identification of proteomic expression profile in human lymph and plasma

To obtain a comprehensive comparative proteomic characterization of the human lymph and matched plasma samples, we carried out 1D SDS–PAGE coupled with nanoLC–ESI–MS/MS analysis of the two biological fluids. Two types of samples were processed: a combined pool of matched lymph and pooled plasma collected from eighteen healthy patients; and a matched set of individual lymph and plasma fluids collected from nine individuals. The limited amounts of lymph collected from the additional nine of the eighteen subjects restricted us from processing them individually (Fig. 2A and B).

All of the lymph and plasma samples were first immunodepleted of IgGs and albumin, and 70 μg of total protein were separated on a 4–20% 1D SDS–PAGE. One representative set of 1DE gels (out of three) are shown in Fig. 2A and B. After staining with Coomassie/Colloidal Blue R-250, the whole gel lane was cut from each lymph and plasma lane and after in-gel-trypsin digestion, peptides were analyzed by nanoLC–ESI–MS/MS using either the LTQ or Orbitrap mass spectrometers. Three independent 1DEF coupled with nanoLC MS/MS proteomics assays were run, two of which were processed with the nanoLC LTQ and one with the Orbitrap system.

Supplement Table 2 list all the non-redundant identified proteins using the criteria described in the Materials and methods section. The list is based on the protein hits derived from the pooled eighteen samples and nine individual subjects, analyzed by both LTQ and Orbitrap nanoLC ESI MS/MS. A total of 253 proteins (Supplement Table 2A) were considered to be positively identified ($p<0.05$) and 14 proteins are reported as unknowns (Supplement Table 2B) (albumins, all classes of immunoglobulins, keratins and trypsin fragments contaminants are excluded from both Supplement Table 2 and the final IPA analysis). The proteins previoussly reported in the HUPO Plasma Proteome Project [14] are marked. The entries which were not previously reported [14] are shadowed. One hundred forty four proteins are common between the lymph and plasma samples, while the distinctive/enriched proteomes of lymph and plasma is represented by 72 and 37 proteins, respectively (Venn diagram is shown in Fig. 2C).

Further analysis of the cellular distribution of the common proteome presented in Supplement Table 2 indicated that the majority (76%) of shared proteins was soluble extracellular proteins and only a few were derived from intracellular organelles, such as 2% from nucleus, 9% from the cytosol and 8% from the plasma membrane (Fig. 2D). On a functional level, over 50% of the common extracellular proteome was represented by the complement system, transporters, metabolism regulators and protease inhibitors (Supplement Table 2A and Fig. 3A). The common proteome of the human lymph and plasma was further classified by the IPA analysis to major functional networks associated with the hematological system development and function (24%), immunological and hematological disease (23%), humoral and inflammatory response (15%) and cellular movement activities (12%). Small molecule biochemistry, vitamin and mineral metabolism, cell signaling and the rest of the cellular metabolism (carbohydrate, nucleic acids, DNA replication) were represented by 25% of the total common proteome (Fig. 3A). Several of these proteins were previously characterized by other groups as “canonical protein sequences from plasma”, and are included in the Human Plasma Peptide Atlas [14]. These included beta-actin, polipoprotein A-IV, apolipoprotein B, apolipoprotein D, apolipo-protein E, biotinidase, complement C7, apolipoprotein L1, complement C3, complement C1q subcomponent subunit C, lacto/transferrin, complement C1q and many others from the apolipoproteins family, complement system, serpin inhibitors, and coagulation factors [36–38].

Analysis of the distinctive proteomes of the pooled lymph and plasma (Fig. 2E, F) indicated a partial skewing of the lymph proteome towards intracellular proteins (25% extracellular, 32% cytoplasm, 21% nucleus and 11% plasma membrane) and the plasma proteome towards plasma membrane and extracellular proteins (45% extracellular, 12% plasma membrane, 17% cytoplasm and 8% nucleus) (Fig. 2E, F). Further, notable differences appeared when the distinctive proteomes for lymph and plasma were broken down into functional networks derived from IPA analysis (Fig. 3). The analysis of the distinctive “functional proteomics fingerprints” of each fluid highlighted the fact that the proteome of human lymph was characterized by a high abundance of proteins grouped in the “connective tissue development and function” network (up to 40% of the total lymph proteome) (Fig. 3B). Most of the proteins included in this major functional network are derived from the processing of extracellular matrix (ECM) proteins (collagens, cartilage and other ECM proteins (Supplement Table 2A)). Notably, the collagens made at least 10% from the total of the ECM protein content. Another major functional network associated with the distinctive lymph proteome is related to the dermatological disease and other metabolic disorders (31%) followed by the combined networks describing the small molecule biochemistry and posttranslational modifications, cellular signaling and interactions and gene expression and RNA metabolism (29% from the total distinctive lymph proteome) (Fig. 3B).

With respect to the sub-cellular distribution of distinctive proteomes characterizing lymph and plasma (Supplement Table 2A), the lymph contained a higher percentage of intracellular proteins than plasma (54% vs. 25%) (Fig. 3B and C). Additionally, most of the intracellular proteins found in lymph consisted of soluble cytosolic enzymes, cytoskeleton related proteins, ribosomal, translation factors, histones and transcription factors, and to a lesser extent Golgi and mitochondria-derived proteins (Fig. 3B and Supplement Table 2A).

One significant molecular signature characterizing the lymph is the relative enhancement of proteins derived from the nuclear content, especially histones (>5.5%), and splicing and transcription factors (>3%) (Supplement Table 2A and Fig. 3B). Another significant feature for the lymph distinctive proteome is the presence of proteins involved in the translation and protein synthesis pathways (about 7%).

The presence of proteins derived from different subcellular compartments (nucleus, mitochondria, cytosol, plasma membrane and others organelles) was already reported to date in the plasma proteome ([14] — HUPO plasma proteomic project). Thus, our comparative proteomic of lymph and plasma presented here indicates a relative increase of these proteins in the lymph.

By comparison, plasma has less than 1% of protein hits that were derived from ECM catabolism (Supplement Table 2A — proteins marked for plasma) and has very few proteins derived from the intracellular metabolism, protein synthesis and regulation of gene expression. The functional networks associated with the plasma distinctive proteome are very similar with those associated with the common proteome (Fig. 3); namely about 61% of the proteins are involved in the coagulation, lipid transport and metabolism and small molecule biochemistry (18%), and other cellular metabolic functions (17%). These functional networks associated with the distinctive proteome of plasma are partially reflected in the common proteome (Fig. 3C).

### 3.3. Pathway analysis of the proteomes associated with human lymph and plasma

As a further step employed to explore the distinctive proteomic profiles, human plasma and lymph were subjected to IPA analysis to determine the functional networks. IPA analysis was applied to two main sample categories: (i) the distinctive and the common proteomes of lymph and plasma derived both from the pooled (18 patients) and the 9 individual samples (Supplement Table 2 and Fig. 3), and (ii) the upregulated proteins found in the lymph as compared with plasma and derived from 2D-DIGE analysis (Table 1, Fig. 4A, B and C).

IPA analysis of the protein hits shown in Table 1 (upregulated proteins in lymph vs. plasma based on 2D DIGE analysis) complemented the analysis of the distinctive lymph proteome revealed from 1DEF. The three major networks associated with these hits are represented by cell death/cancer, dermatological disease and conditions (network 1, Fig. 4 A, Supplement Table 3), cell–cell signaling and lipid metabolism (Fig. 4 B), cellular movement and small molecule biochemistry (Fig. 4C and Supplement Table 3) supporting the view that the lymph carries a significant fraction of the cellular proteome derived from different catabolic functions.

### 3.4. Western blot validation of twenty proteins identified from nanoLC–ESI–MS/MS analysis

To validate our proteomic results, we measured the level of expression for twenty selected protein targets in human pre-nodal lymph and compared them with the matched plasma samples, by Western blotting. We selected to validate proteins already shown to be up-regulated in lymph based on the combined proteomics and IPA analyses, from both the 2D-DIGE and 1DEF nanoLC–ESI/MS/MS assays (9 identified from 2D-DIGE and 11 detected by 1DEF). These identified proteins were mostly from extracellular matrix turn-over (such as collagens, cartilage oligomeric protein, ECM-1, among others) or intracellular pathways and organelles. Equal amounts of lymph and plasma samples were loaded on a 4–20% SDS–PAGE and analyzed by Western blot (Fig. 5). In order to assess the variability of protein expression among the different subjects, as compared with the pooled-samples of 18 healthy donors, we analyzed four individual lymph and matched plasma samples as well (Fig. 5 and Supplementary Fig. 2). Western blot analysis validated that all the extracellular matrix proteins (collagen type I, ECM-1, COMP and lumican) found to be up-regulated, by MS/MS, were also up-regulated in the lymph from both pooled samples and individual subjects (Fig. 5A). All these proteins were previously reported in the rodent and human mesentheric lymph [12,38,39], and in the HUPO atlas for human plasma [14]. Western blot analysis also confirmed the up-regulation of plasma membrane and intracellular proteins in the lymph as

compared with matched plasma, (histones H1E and H2B, ribosomal L22, annexin 6, actin, gelsolin, galectin 7, calmodulin, ubiquitin, Hsp70/Hsc-70, caspase 14, cystatin A, glyceraldehyde dehydrogenase, peptidyl-prolyl cis/trans-isomerase Pin4) (Fig. 5B). Some of these proteins (gelsolin, Hsp-70, calmodulin) were already reported as being part of the lymph proteome [12,38,39] and the human plasma [14]. The only protein that we could not validate by Western blot analysis was BAI-1 associated protein 2, which was shown by 2D-DIGE analysis to be at least 8 fold up-regulated in the lymph as compared with plasma from pooled samples from 18 healthy donors (Fig. 1C, Table 1A and Supplement Fig. 3).

## 4. Discussion

The anatomical difficulty of collecting human lymph samples from normal volunteers has constituted a major barrier to the characterization of this biological fluid. Thus the extent to which the composition of the lymph proteome reflects that of the plasma has remained unanswered for many decades. Leak et al. [6] were the first to provide a proteomic comparison between bovine lymph and plasma using MS/MS analysis performed on differentially expressed protein spots collected from comparative 2D PAGE gels. Their analysis showed for the first time that the lymph proteome contained proteins that were unique to lymph. Major proteins found in lymph, but also at lower concentrations in plasma, included fibrinogen α-and β-chains, immunoglobulin (IgG), serotransferrin precursor, lactoferrin, and apolipoprotein A-1. Two proteins that were identified as uniquely expressed in lymph were glial fibrillary acidic protein and neutrophil cytosol factor-1 [6]. A report from our laboratory on the lymph and plasma peptidome also showed a difference between pre-nodal lymph and matched plasma in the amount of processed protein fragments and peptides found in the former compared with the latter [13]. Analysis of the lymph peptidome indicated that processed peptides were derived from cellular cytosolic and organelle proteins, extracellular proteins, and plasma membrane-associated proteins [13]. This analysis highlighted for the first time the notion that the proteome/peptidome of the lymph contained not only proteins derived from plasma proteins, but also proteins and peptides derived from the metabolism/catabolism of parenchymal organs, connective tissue remodeling, and secretion products derived from cells circulating in the lymph [7-9]. The lymphatic endothelium was also shown to contribute to an array of proteins and cytokines in the lymph, which remain to be fully characterized [9].

As it passes from capillary to lymphatics, the lymph is in direct contact with each cellular layer of the parenchymal organs, suggesting that the expression profile of the lymph could be uniquely defined by the anatomical region from which it was derived [1–4]. Earlier studies in animals have lent some support to this notion. For example, lymph proteomics reported by Goldfinch et al. [13] provided a comprehensive view of the sheep gastric lymph in response to infection with the parasitic nematode *Teladorsagia circumcincta*. 2D gel analysis followed by MALDI-TOF and MS/MS determined a significant increase of gelsolin, α-1 β glycoprotein and hemopexin in the lymph collected from infected animals as compared with healthy controls [12]. Another proteomics analysis examined the mesenteric lymph from Wistar rats under physiological conditions or following induction of pancreatitis [11]. This proteomic analysis reported two hundred and forty-five proteins, including 35 hypothetical proteins, uniquely expressed in the mesenteric lymph of rats with pancreatitis [11]. Eight of the 245 proteins had a significant increase in their relative abundance in acute pancreatitis conditioned mesenteric lymph, and 7 of these were pancreatic catabolic enzymes (pancreatic amylase 2, pancreatic lipase, carboxypeptidase A2, chymotrypsinogen B, carboxypeptidase B1, cationic trypsinogen, ribonuclease 1).

As an extension of the already described self-peptidome of the human lymph [13], we characterized the protein expression profile of human pre-nodal afferent lymph compared to

matching plasma samples. Since the accuracy of finding new protein markers associated with lymph and plasma depended on the amount of starting material and on the sensitivity of the mass spectrometric methods employed, we considered it more relevant for a first comparison of the lymph-plasma proteomics to combine samples of healthy donors rather than performing an analysis on individual patients [13]. However, in order to confirm the "common" proteome that could be shared between these biological fluids and to further discover new "markers" of the potential "enriched" proteome of lymph and plasma, we further processed and analyzed nine healthy individual patients, each having lymph and matched plasma.

A combination of two-dimensional fluorescence difference in gel electrophoresis (2D-DIGE) and one dimensional SDS–PAGE coupled with nanoLC–ESI–MS/MS was employed to determine the proteomic signature of the two pooled biological samples and of each of the individual lymph and plasma collected from 9 patients [27,28,31,32,35,38].

The 1DEF nanoLC–MS/MS analysis of the protein expression profiles of human lymph and plasma identified some differences between the samples: (i) consistent with the notion that the lymph carries apoptotic cells and products of organ and cellular catabolism, the number of proteins derived from intracellular sources (ribosomes, ER, mitochondria, cytoskeleton and cytoplasm) were significantly more abundant in the lymph proteome (54%) than in the plasma one (25%), and (ii) fragments of extracellular matrix proteins (such as collagens) derived from organ remodeling were also more frequently represented in the lymph proteome (10%) as compared with plasma (<1%). As expected, the analysis of individual matched human lymph and plasma from nine healthy subjects and the pooled biological fluids samples from eighteen healthy donors revealed a conserved "core" of proteins shared between the these two biological fluids. Notably, the total number of unique peptides and percentage sequence coverage analysis ($p<0.05$) showed that some of the hits in the "common" repertoire had a higher differential expression in the lymph vs. plasma (Table 2A).

Similarly, the comparative proteomic analysis using 2D-DIGE analysis showed for the first time that the human pre-nodal lymph is characterized by an enriched set of proteins such as: alpha-1-antitrypsin, annexin A1, alpha-tubulin, cystatin A, BAI-1 associated protein 2, calmodulin-like protein, caspase 14, C-type lectin domain family 3, desmoglein-1, fatty acid binding protein, gelsolin, glutathione S-transferase, pepsin-like aspartate protease, S-100 A9 $Ca^{2+}$ binding protein, and vitamin D binding protein. Many of these proteins were previously reported in the plasma as well [14,15], however, in our analysis they were consistently higher (at least four fold higher) in lymph as compared with plasma (three independent experiments, $p<0.05$). Few other proteins consistently showed highly enriched expression in lymph as compared with plasma (cartilage oligomeric matrix protein, histones family, splicing factors, elongation factors, ribosomal proteins, cystatin C, Protein S (alpha) and lectin, galactoside-bindingbinding protein) [15].

When compared with the published proteomes of the rodent and human post-shock mesenteric lymph [35–38], we found from our 1DEF and 2D-DIGE proteomic profiles that more than 90% of the proteins reported in the pre-shock mesenteric lymph are also present in the prenodal healthy lymph (see Table 2A).

In conclusion, this is the first analysis of human lymph that establishes, in a semi-quantitative manner, that the lymph proteome is comprised of a series of proteins which derive from the catabolism of parenchymal cells and the remodeling of the extracellular matrix, which are less represented in plasma. The enrichment of tissue proteins in the pre nodal lymph versus the plasma likely reflect the filtration process of the lymph nodes which

deplete the lymph from tissue specific antigens, before entering the thoracic duct and then major blood vessels.

The comparison between the proteomic profiles should not be interpreted as the final fingerprint of the two biological fluids since it is important to point out that the inherent sensitivity of the analytical platform precluded the identification of many bioactive components such as cytokines, and low abundant proteins which could further define this important biological fluids.

## Supplementary Material

Refer to Web version on PubMed Central for supplementary material.

## Acknowledgments

We would like to thank the Laboratory for Macromolecular Analysis and Proteomic at Albert Einstein College of Medicine, for the mass spectrometry data acquisition (NIH grant 1S10RR019352). Lymph and plasma proteomic analysis using the Orbitrap Velos was performed at MS Bioworks, LLC, Ann Arbor, MI.

## References

1. Heim, WJ. On the chemical composition of lymph from subcutaneous vessels. Cambridge, Mass: Harvard University Press; 1932. p. 553-8.
2. Sixt M, Kanazawa N, Selg M, Samson T, Roos G, Reinhardt DP, et al. The conduit system transports soluble antigens from the afferent lymph to resident dendritic cells in the T cell area of the lymph node. Immunity. 2005; 22:19–29. [PubMed: 15664156]
3. Roozendaal R, Mempel TR, Pitcher LA, Gonzalez SA, Verschoor S. Conduits mediate transport of low-molecular-weight antigen to lymph node follicles. Immunity. 2009; 30:264–76. [PubMed: 19185517]
4. Gretz JE, Kaldjian EP, Anderson AO, Shaw S. Sophisticated strategies for information encounter in the lymph node: the reticular network as a conduit of soluble information and a highway for cell traffic. J Immunol. 1996; 157:495–9. [PubMed: 8752893]
5. Leak LV, Liotta LA, Krutzsch H, Jones M, Fusaro VS, Ross SJ, et al. Proteomic analysis of lymph. Proteomics. 2004; 4:753–65. [PubMed: 14997497]
6. Interewicz B, Olszewski WL, Leak LV, Petricoin EF, Liotta LA. Profiling of normal human leg lymph proteins using the 2-D electrophoresis and SELDI-TOF mass spectrophotometry approach. Lymphology. 2004; 37:65–72. [PubMed: 15328759]
7. Nanjee MN, Cooke CJ, Olszewski WL, Miller NL. Lipid and apolipoprotein concentrations in prenodal leg lymph of fasted humans. Associations with plasma concentrations in normal subjects, lipoprotein lipase deficiency, and LCAT deficiency. J Lipid Res. 2000; 41:1317–27. [PubMed: 10946020]
8. Olszewski WL, Pazdur J, Kubasiewicz E, Zaleska M, Cooke CJ, Miller NE. Lymph draining from foot joints in rheumatoid arthritis provides insight into local cytokine and chemokine production and transport to lymph nodes. Arthritis Rheum. 2001; 44:541–9. [PubMed: 11263768]
9. Knight JS, Baird DB, Hein WR, Pernthaner A. The gastrointestinal nematode Trichostrongylus colubriformis down-regulates immune gene expression in migratory cells in afferent lymph. BMC Immunol. 2010; 11:51. [PubMed: 20950493]
10. Peltz ED, Moore EE, Zurawel AA, Jordan JR, Damle SS, Redzic JS, et al. Proteome and system ontology of hemorrhagic shock: exploring early constitutive changes in postshock mesenteric lymph. Surgery. 2009; 146(2):347–57. [PubMed: 19628095]
11. Mittal A, Middleditch M, Ruggiero K, Buchanan CM, Jullig M, Loveday B, et al. The proteome of rodent mesenteric lymph. Am J Physiol Gastrointest Liver Physiol. 2008; 295(5):G895–903. [PubMed: 18772360]

12. Goldfinch GM, Smith WD, Imrie L, McLean K, Inglis NF, Pemberton AD. The proteome of gastric lymph in normal and nematode infected sheep. Proteomics. 2008; 8(9):1909–18. [PubMed: 18384101]

13. Clement CC, Cannizzo ES, Nastke MD, Sahu R, Olszewski W, Miller NE, et al. An expanded self-antigen peptidome is carried by the human lymph as compared to the plasma. PLoS One. Mar 26.2010 5(3):e9863. [PubMed: 20360855]

14. Omenn GS, States DJ, Adamski M, Blackwell TW, Menon R, Hermjakob H, et al. Overview of the HUPO Plasma Proteome Project: results from the pilot phase with 35 collaborating laboratories and multiple analytical groups, generating a core dataset of 3020 proteins and a publicly-available database. Proteomics. 2005; 13:3226–45. [PubMed: 16104056]

15. Shen Z, Want EJ, Chen W, Keating W, Nussbaumer W, Moore R, et al. Sepsis plasma protein profiling with immunodepletion, three-dimensional liquid chromatography tandem mass spectrometry, and spectrum counting. J Proteome Res. 2006; 5:3154–60. [PubMed: 17081067]

16. Echan LA, Tang HY, Li-Khan N, Lee K, Speicher DW. Depletion of multiple high-abundance proteins improves protein profiling capacities of human serum and plasma. Proteomics. 2005; 13:3292–303. [PubMed: 16052620]

17. Hinerfeld D, Innamorati D, Pirro J, Tam SW. Serum/plasma depletion with chicken immunoglobulin Y antibodies for proteomic analysis from multiple Mammalian species. J Biomol Tech. 2004; 3:184–90. [PubMed: 15331584]

18. Tannu NS, Hemby SE. Two-dimensional fluorescence difference gel electrophoresis for comparative proteomics profiling. Nat Protoc. 2006; 1:1732–42. [PubMed: 17487156]

19. Chen C, Boylan MT, Evans CA, Whetton AD, Wright EG. Application of two-dimensional difference gel electrophoresis to studying bone marrow macrophages and their in vivo responses to ionizing radiation. J Proteome Res. 2005; 4:1371–80. [PubMed: 16083289]

20. Yu KH, Rustgi AK, Blair IA. Characterization of proteins in human pancreatic cancer serum using differential gel electrophoresis and tandem mass spectrometry. J Proteome Res. 2005; 4:1742–51. [PubMed: 16212428]

21. Gharbi S, Gaffney P, Yang A, Zvelebil MJ, Cramer R, Waterfield MD, et al. Evaluation of two-dimensional differential gel electrophoresis for proteomic expression analysis of a model breast cancer cell system. Mol Cell Proteomics. 2002; 1:91–8. [PubMed: 12096126]

22. Kall L, Storey JD, MacCoss MJ, Noble SW. Assigning significance to peptides identified by tandem mass spectrometry using decoy databases. J Proteome Res. 2008; 7:29–34. [PubMed: 18067246]

23. Gupta N, Pevzner PA. False discovery rates of protein identifications: a strike against the two-peptide rule. J Proteome Res. 2009; 8:4173–81. [PubMed: 19627159]

24. Viner, R.; Zhang, T.; Peterman, S.; Zabrouskov, V. Application Note 386. ThermoScientific; 2009. Advantages of the LTQ Orbitrap for protein identification in complex digests.

25. Che, FY.; Madrid-Aliste, C.; Burd, B.; Zhang, H.; Nieves, E.; Kim, K., et al. Comprehensive proteomic analysis of membrane proteins in *Toxoplasma gondii*. Mol Cell Proteomics. 2010. http://dx.doi.org/10.1074/mcp.M110.000745

26. Keller A, Nesvizhskii AI, Kolker E, Aebersold R. Empirical statistical model to estimate the accuracy of peptide identifications made by MS/MS and database search. Anal Chem. 2002; 74(20):5383–92. [PubMed: 12403597]

27. Nesvizhskii AI. A statistical model for identifying proteins by tandem mass spectrometry. Anal Chem. 2003; 75(17):4646–58. [PubMed: 14632076]

28. Clement CC, Rotzschke O, Santambrogio L. The lymph as a pool of self-antigens. Trends Immunol. 2011; 32(1):6–11. [PubMed: 21123113]

29. Galeva N, Altermann M. Comparison of one-dimensional and two-dimensional gel electrophoresis as a separation tool for proteomic analysis of rat liver microsomes: cytochromes P450 and other membrane proteins. Proteomics. 2002; 2:713–22. [PubMed: 12112853]

30. Piersma SR, Fiedler U, Span S, Lingnau A, Pham TV, Hoffmann S, et al. Workflow comparison for label-free, quantitative secretome proteomics for cancer biomarker discovery: method evaluation, differential analysis, and verification in serum. J Proteome Res. 2010; 9(4):1913–22. [PubMed: 20085282]

31. Ahn S-M, Simpson RJ. Body fluid proteomics: prospects for biomarker discovery. Proteomics Clin Appl. 2007; 1(9):1004–15. [PubMed: 21136753]
32. Meng Z, Veenstra TD. Proteomic analysis of serum, plasma, and lymph for the identification of biomarkers. Proteomics Clin Appl. 2007; 1(8):747–57. [PubMed: 21136731]
33. Armandola EA. Proteome profiling in body fluids and in cancer cell signaling. MedGenMed. 2003; 5(2):18. [PubMed: 14603117]
34. Whiteaker JR, Zhang H, Eng JK, Fang R, Piening BD, Feng LC, et al. Head-to-head comparison of serum fractionation techniques. J Proteome Res. 2007; 6:828–36. [PubMed: 17269739]
35. Zurawel A, Moore Ernest E, Peltz Erik D, Jordan Janeen R, Damle Sagar, Dzieciatkowska Monika, et al. Proteomic profiling of the mesenteric lymph after hemorrhagic shock: differential gel electrophoresis and mass spectrometry analysis. Clin Proteomics. 2011; 8(1):1–14. [PubMed: 21906351]
36. Anderson NL, Polanski M, Pieper R, Gatlin T, Tirumalai RS, Conrads TP, et al. The human plasma proteome: a nonredundant list developed by combination of four separate sources. Mol Cell Proteomics. 2004; 3:311–26. [PubMed: 14718574]
37. Farrah T, Deutsch EW, Omenn GS, Campbell DS, Sun Z, Bletz JA, et al. A high confidence human plasma proteome reference set with estimated concentrations in PeptideAtlas. Mol Cell Proteomics. 2011; 10(9):6353–14.
38. Dzieciatkowska, Monika; Wohlauer Max, V.; Moore Ernest, E.; Damle, Sagar; Peltz, Erik; Campsen, Jeffrey, et al. Proteomic analysis of human mesenteric lymph. Shock. Apr; 2011 35(4): 331–8. [PubMed: 21192285]
39. Liu T, Qian WJ, Gritsenko MA, Xiao W, Moldawer LL, Kaushal A, et al. High dynamic range characterization of the trauma patient plasma proteome. Mol Cell Proteomics. 2006; 5:1899–913. [PubMed: 16684767]

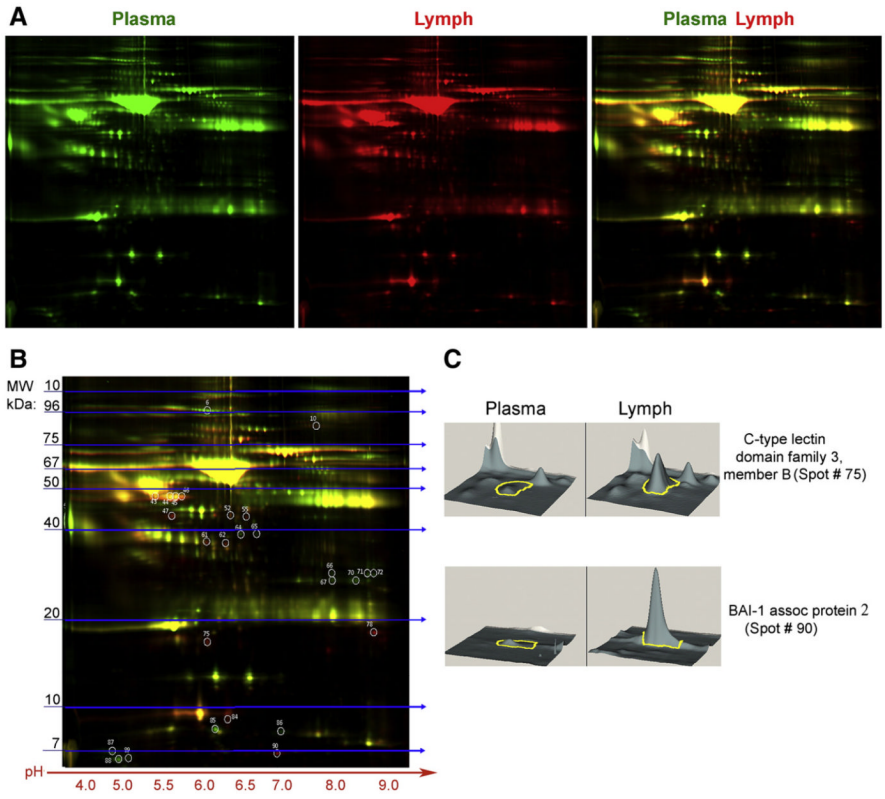


**Fig. 1.**

Comparative 2D-DIGE proteomics profiles of human lymph and plasma. A) 2D-DIGE image of proteins expressed in plasma (Cy3 green fluorescence) and lymph (Cy5 red fluorescence). One out of three independent experiments is shown. (B) 2D-DIGE of differentially expressed lymph and plasma proteins. The green spots represent proteins up-regulated in plasma while red spots indicate proteins up-regulated in lymph. Circles indicate proteins having at least a 3.0 fold change in fluorescence expression index (defined as the ratio lymph/plasma). These proteins were excised from the gel and subjected to nanoLC–ESI–MS/MS analysis. Nineteen protein spots were selected with a lymph/plasma ratio above 4.2 and are presented in Table 1 (11 spots are displayed in Fig. 1B and 8 spots are displayed in Supplementary Fig. 1). Proteins with at least a 3.0 fold change in the lymph/plasma fluorescence index are presented in Supplementary Table 1. (C) 3D view of individual spots of proteins significantly up-regulated (≥+8.0 fold change) in the lymph as compared with the plasma following analysis using DeCyder software. Each protein is also reported in Table 1. The up-regulation of tetranectin (CLEC3B) expression in the lymph as compared with plasma was validated by Western analysis (Fig. 5). BAI-1 associated protein 2 was not yet validated by Western blot but its major unique peptide MS/MS fragmentation profile is included in Supplementary Fig. 3.

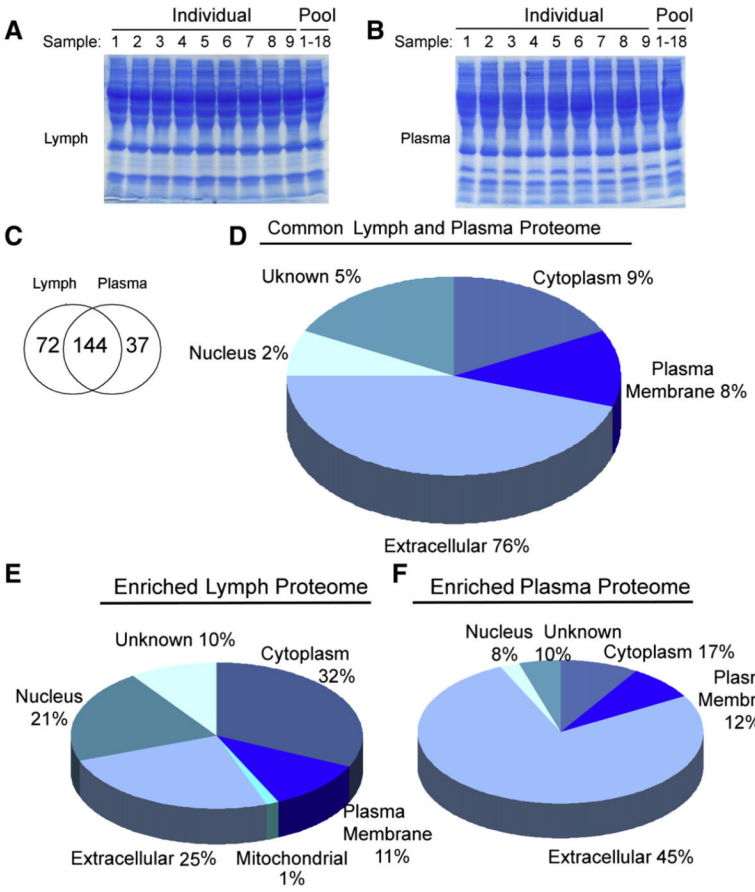


**Fig. 2.**

Analysis of the human lymph and plasma proteomes using 1DE SDS–PAGE coupled with nanoLC tandem MS/MS. A) Coomassie stained 4–15% SDS–PAGE of human lymph (9 individual patients and pooled sample from 18 patients) and B) human plasma (9 individual patients and pooled sample from 18 patients) (70 μg of total protein were run in each lane). Sixteen gel bands were excised from each lane; proteins were tryptic-digested and analyzed by nanoLC–ESI–MS/MS analysis. C) Venn diagram analysis of the proteomics profiles derived from 18 pooled lymph and matched plasma samples and from the combined analysis of 9 individual lymph and plasma samples (the non-redundant list of all proteins found in the lymph and plasma is shown in Table 2). D, E, F) Pie charts displaying the subcellular distribution of the D) lymph and plasma common proteome displayed in the Venn diagram (144 shared proteins). Numbers are calculated as percentage of the common 144 proteins (Table 2). Cellular distribution of the enriched proteomes found in the E) lymph and in the F) plasma (72 and 37 enriched proteins in the lymph and plasma respectively). Numbers are calculated as percentage of each enriched proteome. The proteins associated with the common 144 and the enriched proteins are shown in Table 2 (unknowns are included in the % distribution).

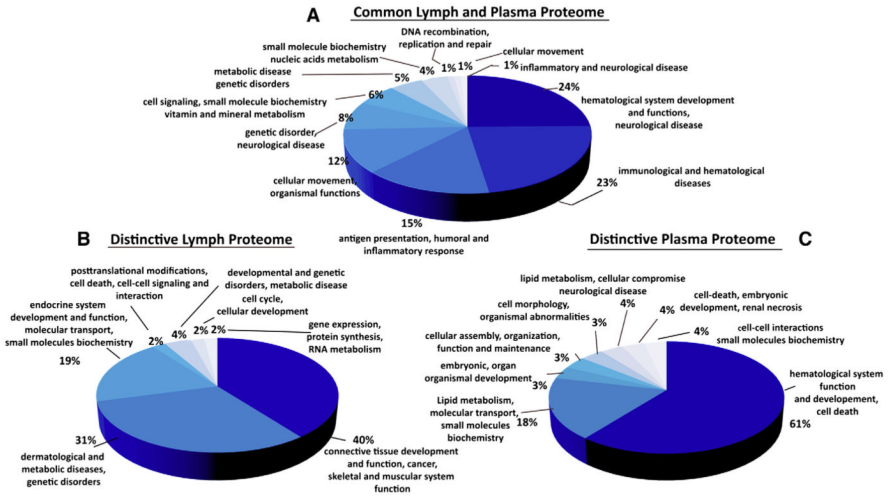


**Fig. 3.**

Functional networks analysis of the human lymph and plasma common and enriched proteomes. A) Pie chart of the human lymph and plasma major common functional networks. Data were generated using the IPA (ingenuity pathway analysis) software. The graphic display is generated from the common 144 proteins shown in Table 2. B) Pie chart of the human major lymph networks derived from the enriched lymph proteome is shown in Fig. 2C (72 proteins) and Table 2. C) Pie chart of the human major plasma functional networks derived from the enriched plasma proteome shown in Fig. 2C (32 proteins) and Table 2.

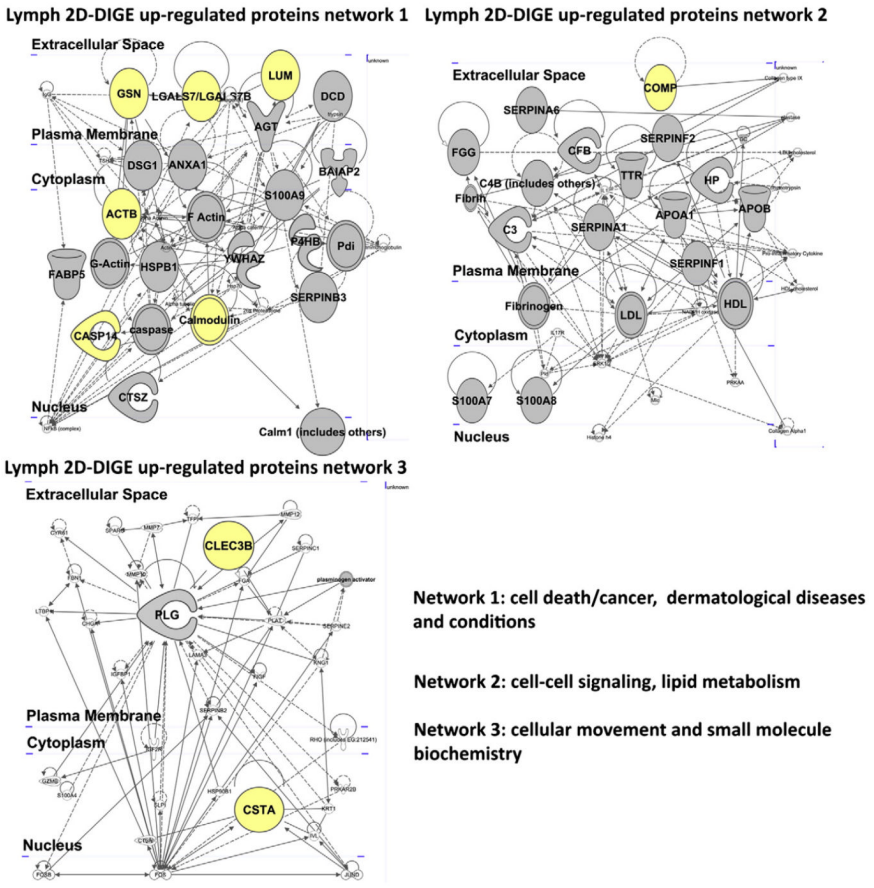


**Fig. 4.**

Network analysis of the proteins up-regulated in the lymph as detected by 2D-DIGE. Graphic display of the human lymph major networks, compiled from the list of proteins presented in Table 1 (A and B). Lists of the genes names and proteins analyzed in the networks are reported in Supplementary Table 2. Highlighted in yellow are the hits validate by Western blot analysis shown in Fig. 5.

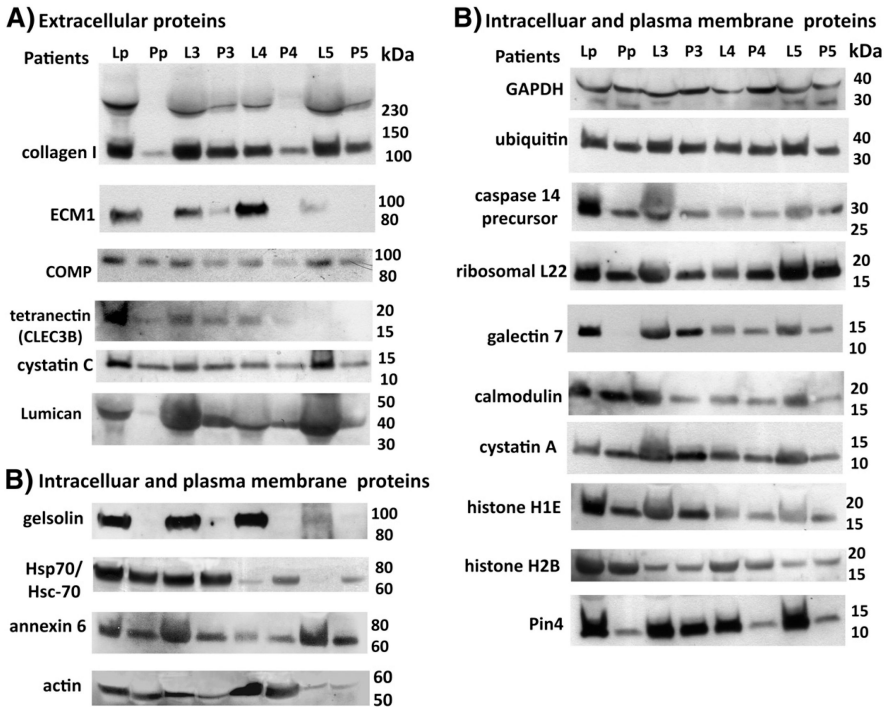


**Fig. 5.**

Western blot analysis of selected lymph proteins. Six major extracellular proteins (A) and 14 intracellular and plasma membrane associated proteins (B), found to be expressed at higher level in the lymph vs. the plasma, were validated by Western blot analysis. Lp and Pp indicate pooled samples of lymph and plasma, respectively, from 18 healthy donors. L3–L5 and P3–P5 are individual samples from lymph and plasma, from different donors.

## Table 1

List of proteins up-regulated in the lymph vs. plasma.

| | Ratio of lymph to plasma *(b)* | Protein name | GI accession number *(c)* | MW (kDa) predicted | Observed MW (kDa) 2D-DIGE | pI predicted | Observed pI 2D-DIGE | Mascot protein score *(d)* | % seq coverage | emPAI *(e)* |
|---|---|---|---|---|---|---|---|---|---|---|
| *2D-DIGE(*Fig. 1*)spot ID # (a)* | | | | | | | | | | |
| 44 | 4.4 | Serum vitamin D-binding protein | 181482 | 54.52 | 48.5 | 5.4 | 5.5 | 1856 | 58% | 12.65 |
| | | Alpha-1-Antitrypsin | 1942629 | 46.87 | | 5.37 | | 495 | 64% | 4.66 |
| | | Antgiotensinogen | 15079348 | 53.40 | | 5.87 | | 101 | 19% | 0.08 |
| | | Apolipoprotein A-I | 90108664 | 30.76 | | 5.56 | | 77 | 19% | 0.14 |
| | | Fibrinogen gamma chain | 119625320 | 52.10 | | 5.37 | | 99 | 22% | 0.08 |
| 45 | 4.4 | Vitamin D Binding Protein | 18655424 | 54.52 | 48.5 | 5.4 | 5.6 | 2091 | 61% | 8.40 |
| | | Alpha-1-antitrypsin | 177827 | 46.78 | | 5.37 | | 218 | 35% | 0.83 |
| | | Fibrinogen gamma chain | 119625320 | 52.10 | | 5.37 | | 91 | 26% | 0.37 |
| | | Fetuin-B | 119598591 | 42.88 | | 6.46 | | 108 | 25% | 0.33 |
| | | Apolipoprotein AI | 90108664 | 30.75 | | 5.56 | | 51 | 22% | 0.3 |
| | | **Lumican** | **4505047** | **38.74** | | **6.16** | | **57** | **16%** | **0.11** |
| 46 | 4.5 | Vitamin D Binding Protein | 18655424 | 54.52 | 48.5 | 5.4 | 5.7 | 1553 | 45% | 5.47 |
| | | Alpha-1-antitrypsin | 1942629 | 46.87 | | 5.37 | | 132 | 18% | 0.41 |
| | | Angiotensinogen | 15079348 | 53.40 | | 5.87 | | 118 | 11% | 0.26 |
| | | C4B3 | 40737343 | 47.93 | | 5.78 | | 125 | 9% | 0.07 |
| | | Alpha-2-antiplasmin | 115583663 | 54.87 | | 5.87 | | 61 | 16% | 0.08 |
| | | Apolipoprotein AI | 90108664 | 30.75 | | 5.56 | | 54 | 13% | 0.3 |
| | | Fibrinogen gamma chain | 119625320 | 52.10 | | 5.37 | | 105 | | 0.17 |
| | | Prothrombin | 339641 | 71.47 | | 5.64 | | 53 | 13% | 0.12 |
| 47 | 8.9 | Vitamin D Binding Protein | 28373620 | 54.52 | 45.5 | 5.4 | 5.5 | 377 | 34% | 0.96 |
| | | Fibrinogen gamma chain | 182439 | 52.10 | | 5.37 | | 106 | 13% | 0.17 |
| | | Haptoglobin | 119579598 | 45.86 | | 6.13 | | 88 | 8% | 0.19 |
| | | Alpha-1-antitrypsin | 1942629 | 46.87 | | 5.37 | | 61 | 20% | 0.09 |
| 55 | 4.7 | Vitamin D-binding protein precursor | 139641 | 54.52 | 44.5 | 5.4 | 6.5 | 174 | 30% | 0.69 |

| | Ratio of lymph to plasma *(b)* | Protein name | GI accession number *(c)* | MW (kDa) predicted | Observed MW (kDa) 2D-DIGE | pI predicted | Observed pI 2D-DIGE | Mascot protein score *(d)* | % seq coverage | emPAI *(e)* |
|---|---|---|---|---|---|---|---|---|---|---|
| | | Pigment epithelium-derived factor (PEDF) | 39725934 | 46.48 | | 5.97 | | 53 | 2% | 0.09 |
| 61 | 6.6 | Haptoglobin | 1212947 | 45.86 | 38.5 | 6.13 | 6.0 | 148 | 21% | 0.19 |
| | | Cathepsin Z | 27503311 | 34.53 | | 6.70 | | 84 | 7% | 0.12 |
| 62 | 4.8 | Haptoglobin | 1212947 | 45.85 | 38.5 | 6.13 | 6.3 | 297 | 31% | 0.30 |
| | | Apolipoprotein L1 | 3135985 | 44.00 | | 5.60 | | 137 | 12% | 0.32 |
| | | Cathepsin Z | 27503311 | 34.53 | | 6.70 | | 58 | 13% | 0.12 |
| 75 | 8.0 | **CLEC3B (Tetranectin)** | **119585139** | **22.95** | **18.5** | **5.52** | **6.0** | **89** | **49%** | **0.5** |
| 78 | 9.4 | Olfactory receptor 2T35 | 49226830 | 36.70 | 19.0 | 9.03 | 8.5 | 45 | 2% | 0.12 |
| 84 | 6.3 | BAI-1 associated protein 2 | 119610031 | 61.11 | 9.0 | 8.99 | 6.4 | 130 | 32% | 0.07 |
| | | Protein disulfide-isomerase | 20070125 | 57.48 | | 4.76 | | 91 | 10% | 0.07 |
| 90 | 11.5 | BAI-1 associated protein 2 | 119610031 | 61.11 | 7.0 | 8.99 | 6.95 | 56 | 13% | 0.14 |
| *2D-DIGE(*Supplement Fig. 1*)spot ID#* | | | | | | | | | | |
| 1 | 4.9 | **Cartilage oligomeric matrix protein** | **40217843** | **85.43** | **96** | **4.36** | **4.8** | **65** | **11%** | **0.15** |
| | | Desmoglein-1 | 416917 | 113.74 | | 4.90 | | 81 | 15% | 0.11 |
| 3 | 5.4 | **Gelsolin** | **4504165** | **85.7** | **83** | **5.90** | **6.0** | **163** | **12.3%** | **0.33** |
| 4 | 4.2 | Gelsolin | 4504165 | 85.7 | 83 | 5.90 | 6.5 | 69 | 13% | 0.1 |
| 18 | 5.6 | **Caspase 14** | **6912286** | **27.94** | **32** | **5.44** | **6.1** | **82** | **35%** | **0.54** |
| | | Dermicidin | 148271063 | 11.39 | | 6.08 | | 75 | 12% | 0.40 |
| | | Transthyretin | 114318993 | 15.99 | | 5.52 | | 74 | 33% | 0.64 |
| | | S100 calcium-binding protein A9 | 4506773 | 13.24 | | 5.71 | | 72 | 28% | 0.34 |
| | | S100 calcium-binding protein A8 | 13543539 | 10.88 | | 6.51 | | 66 | 19% | 0.43 |
| | | S100 calcium-binding protein A7 | 57547671 | 11.57 | | 6.28 | | 64 | 38% | 0.40 |
| 20a | 28.4 | **Calmodulin-like protein 5** | **8393159** | **15.88** | **20** | **4.34** | **4.4** | **323** | **52%** | **3.44** |
| | | **Caspase 14** | **6912286** | **27.94** | | **5.44** | | **208** | **40%** | **2.65** |
| | | **Cystatin-A** | **6503217** | **11.00** | | **5.38** | | **71** | **47%** | **1.02** |
| | | 14-3-3 protein zeta/delta | 21735625 | 27.89 | | 4.72 | | 55 | 14% | 0.16 |

| | Ratio of lymph to plasma *(b)* | Protein name | GI accession number *(c)* | MW (kDa) predicted | Observed MW (kDa) 2D-DIGE | pI predicted | Observed pI 2D-DIGE | Mascot protein score *(d)* | % seq coverage | emPAI *(e)* |
|---|---|---|---|---|---|---|---|---|---|---|
| | | Transthyretin | 114318993 | 15.99 | | 5.52 | | 52 | 55% | 0.28 |
| 20b | 9.4 | **Calmodulin-like protein 5** | **8393159** | **15.88** | **19** | **4.34** | **4.4** | **60** | **44%** | **0.64** |
| | | **Cystatin-A** | **6503217** | **11.0** | | **5.38** | | **55** | **12%** | **0.42** |
| 20c | 14.1 | S100 calcium-binding protein A9 | 4506773 | 13.24 | 19 | 5.71 | 4.9 | 908 | 65% | 13.06 |
| | | S100 calcium-binding protein A8 | 13543539 | 10.88 | | 6.51 | | 454 | 45% | 3.15 |
| | | Calmodulin-like | 8393159 | 15.90 | | 4.31 | | 248 | 87% | 1.11 |
| | | protein 5 | | | | | | | | |
| | | Serpin B3 | 5902072 | 44.59 | | 6.35 | | 434 | 65% | 2.91 |
| | | **Galectin 7** | **4504985** | **15.12** | | **7.03** | | **404** | **45%** | **1.84** |
| | | **Actin, cytoplasmic -1** | **4501885** | **42.05** | | **5.29** | | **223** | **49%** | **0.78** |
| | | Heat shock protein | 19855073 | 22.82 | | 5.98 | | 156 | 40% | 1.01 |
| | | Beta-1 | | | | | | | | |
| 30 | 7.5 | **Galectin 7** | **4504985** | **15.12** | **7.0** | **7.03** | **7.2** | **165** | **55%** | **1.19** |
| | | Fatty acid-binding protein, epidermal | 4557581 | 15.49 | | 6.60 | | 83 | 74% | 0.66 |
| | | Heat shock protein | 19855073 | 22.82 | | 5.98 | | 133 | 47% | 1.01 |
| | | Beta-1 | | | | | | | | |
| | | Annexin A1 | 4502101 | 38.91 | | 6.57 | | 47 | 34% | 0.11 |

*(a)* Spot # generated by the DeCyder 2-D Differential Analysis Software (V6.0, GE Healthcare).

*(b)* Ratio of protein expression between lymph and plasma.

*(c)* Accession number (NCBInr database).

*(d)* Mascot protein score; protein scores ≥45 indicate identity or extensive homology, $p<0.05$.

*(e)* emPAI values extracted from Mascot analysis for each spot. In bold are proteins validated by Western blot (see Fig. 5).